

Influence of the particle size distribution on the Critical State Properties of Mine Tailings

Luis Vergaray

Georgia Institute of Technology, Atlanta, Georgia, USA

Jorge Macedo

Georgia Institute of Technology, Atlanta, Georgia, USA

Cody Arnold

Georgia Institute of Technology, Atlanta, Georgia, USA

Marcos Arroyo

CIMNE – Universitat Politècnica de Catalunya – BarcelonaTech, Barcelona, Spain

ABSTRACT: Arguably, critical state soil mechanics (CSSM) is now the preeminent methodology for understanding static liquefaction of mine tailings, having been used in the mining industry by the expert panels retained to investigate recent TSF failures. One of the key ingredients of the CSSM framework is the assessment of a critical state line, which separates contractive from dilative states. A critical state line is often defined by a linear relationship and two parameters, namely the altitude of the critical state line at 1 kPa (Γ) and its slope (λ). In this study, we use the TALENG mine tailings database to investigate potential relationships between the particle features and the particle size distribution and the critical state properties. Towards this end, the critical state line is evaluated for a range of mine tailings with broad gradations and compressibility, defining Γ and λ , with known particle size distributions. This information is subsequently used to investigate potential correlations. Insights from the observations are shared, and potential fundamental mechanisms in explaining correlations between the critical state properties and particle features are discussed.

1 INTRODUCTION

The static liquefaction of mine tailings has caused numerous recent tailings storage facility (TSF) failures, such as the 2015 Fundao failure in Brazil, the 2018 Cadia failure in Australia, and the 2019 Brumadinho failure in Brazil. These failures have caused unprecedented devastating consequences for the environment, infrastructure damage, and loss of human life; they have been in the spotlight of the mining, engineering, and environmental communities (e.g., Morgenstern 2018; Jefferies 2021; Been 2015; Santamarina et al. 2019, Kossoff et al. 2014). This recent worldwide TSF failures have triggered international debates regarding the safety of TSF systems and the mechanical response of mine tailings. In this context, Morgenstern (2018) evaluated contributory factors in fifteen TSF incidents, classifying them into engineering, operations, and regulatory factors. Morgenstern's assessment highlighted that engineering (e.g., inadequate understanding of the mechanical response of mine tailings, inadequate site characterization, etc.) is one of the predominant contributory factors. Other experts (e.g., Jefferies 2022; Been 2015) reached conclusions similar to those of Morgenstern (2018), also highlighting the key role of understanding the response of mine tailings. Thus, advancing the geotechnics of mine tailings is crucial for the design and condition assessment of TSFs. This is particularly challenging as mine tailings are man-made geomaterials, generally classified as sandy silt to almost pure silt, and most approaches in geotechnical engineering have been developed for sands and clays; comparatively, very little exists on intermediate materials. Mine tailings are also geologically young materials, with angular grains rather than subrounded and often with lower proportions of quartz than many natural soils; thus, standard geotechnical correlations should not be taken to be applicable to tailings without detailed consideration of these factors.

Previous efforts on understanding the trends in the mechanical response of particulate materials

under monotonic loadings have been mainly focused on sands with low fine contents (e.g., Sadrekarimi, 2014; Jefferies and Been, 2016, Rabbi et al., 2019). In terms of mine tailings, the experimental studies that have evaluated their mechanical response and the associated mechanical parameters are somewhat limited compared to sand materials (e.g., Jefferies and Been 2015; Shuttle and Jefferies 2016; Fourie and Tshabalala 2005; Carrera et al. 2011; Smith et al. 2019; Macedo and Vergaray 2022; Torres-Cruz and Santamarina 2019). These previous studies emphasize that mine tailings have distinctive mechanical properties compared with what is commonly observed in natural soils, i.e., a higher frictional strength, higher dilatancy, and higher compressibility. These differences are attributed to the microstructure and mineralogy peculiar to mine tailings. Even though previous studies provide valuable insights, the tailings community is still actively working to better understand the mechanical behavior of mine tailings (e.g., Macedo et al. 2020), and part of this effort is directed toward increasing the number of case studies of the mechanical response of mine tailings.

In this study, we present trends for mechanical-based parameters that control the response of mine tailings, in the context of the particle size distribution and particle features, which have not been previously explored considering a large set of tailings materials. The trends are presented using results from 64 mine tailings materials, including available data from the TAILENG (Tailings and industrial waste engineering center) database. This study is structured as follows. After the general introduction in Section 1, Section 2 provides a description of the mine tailings database used in this study. We then discuss the influence of material index properties and the critical state line parameters in Section 3. Next, in Section 4, we discuss a novel interpretation of the location of the critical state line in terms of particle properties and packing indices. Section 5 presents the trends of dilatancy of the examined mine tailings and the proportion of particle sizes, sharing salient insights. Finally, Section 7 closes this study by presenting our conclusions.

2 DATABASE

The TAILENG database used in this study consists of 54 different tailings detailed in Macedo and Vergaray (2022, 6 additional recently tested mine tailings and data gathered from recent studies (Fotovvat et al. 2022; Arroyo and Gens 2021). The mine tailings database corresponds to different ores (i.e., gold, iron, silver, copper, zinc, platinum) covering a broad range of fine contents ($FC = 0 - 100\%$), initial confining stress ($20 - 6000\text{ kPa}$), specific gravity ($G_s = 2.63 - 5.01$), and states (i.e., very loose to dense). Figure 1 shows the particle size distribution for the materials considered in this study, separating them by fine contents for easier visualization.

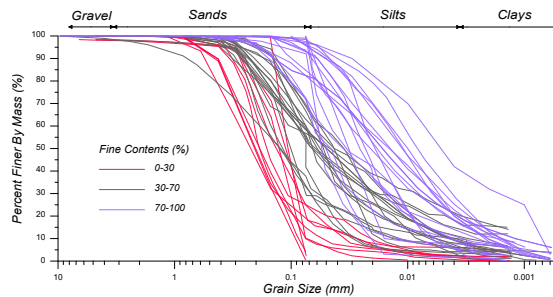


Figure 1. Range of particle size distribution for the materials considered in this study.

3 THE CRITICAL STATE FRAMEWORK

The mechanistic-based parameters under the critical state soil mechanics (CSSM) framework considered here are those related to 1) the description of the CSL in the compression plane, i.e., Γ , λ_e if the CSL is defined in Equation 1 following a Semi-log idealization or a , b , and c for a curved CSL defined in Equation 2, where e_{cs} is the void ratio at the critical state; 2) the description of

stress dilatancy-relations, such as M_{tc} (the critical state stress ratio), and N (volumetric coupling), which are related through Equation 3, where η_{max} is the maximum stress ratio and D_{min} is the maximum dilatancy; 3) the description of state-dilatancy relations, i.e., χ , which relates the maximum dilatancy with the state through Equation 4, where ψ is the state parameter defined by Been and Jefferies (1985); and 4) the description of elastic stiffness, such as A and B , which scales the dependence of G_{max} in terms of mean effective stress (p), e.g., Equation 5, where $F(e)$ represent the functional form proposed by Hardin and Richart (1963) and Pestana and Whittle (1995)

$$e_{cs} = \Gamma - \lambda_e \ln(p) \tag{1}$$

$$e_{cs} = a - b \left(\frac{p}{p_a}\right)^c \tag{2}$$

$$\eta_{max} = M_{tc} + (1 - D_{min})N \tag{3}$$

$$D_{min} = \chi\psi \tag{4}$$

$$G = A \cdot F(e) \cdot (p/p_a)^B \tag{5}$$

It is important to note that Γ , λ_e , M_{tc} , N , χ , and G_{max} are often present as parameters in robust constitutive models, usually formulated for sands (although often named differently or represented by other proxies), and are the basis for the current mechanical-based understanding of static liquefaction (e.g., Jefferies and Been 2015), as also reflected by their use in forensic studies of recent TSF failures (e.g., Morgenstern et al., 2016; Morgenstern et al. 2019; Robertson et al. 2019). One of these models is Norsand (Jefferies 1993), which is selected because of its simplicity as it uses all the mechanistic-based parameters previously discussed and only requires an additional parameter (the plastic modulus, H) that can be assessed during calibrations. Figure 2a shows the estimation of the CSL, Figure 2b shows the η_{max} versus D_{min} plot to estimate M_{tc} and N , Figure 2c shows the state-dilatancy relationship to estimate χ , and Figure 2d shows the G versus p plot to estimate A and B . Hence, once the mechanical parameters (Γ , λ_e , M_{tc} , N , χ , and G_{max}) are assessed, different ranges of responses can be estimated, and static liquefaction becomes just another manifestation of the behavior of a particulate medium.

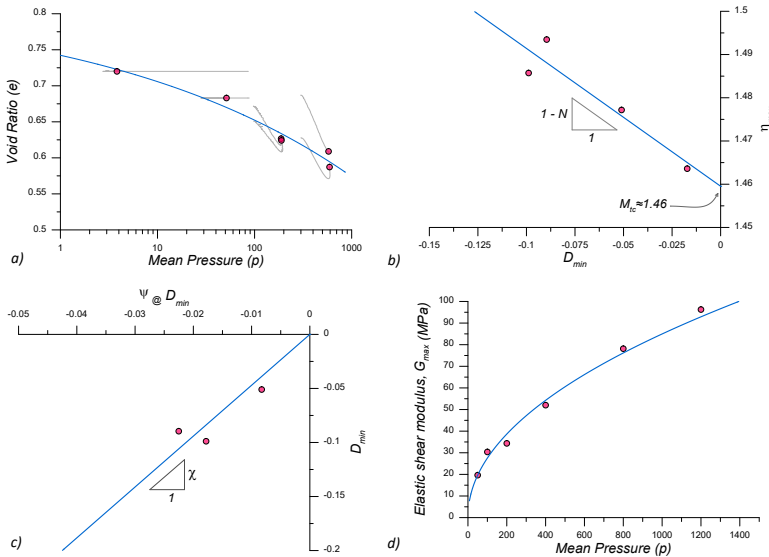


Figure 2. Illustration of the estimation of mechanical-based parameters. a) CSL estimation, b) η_{max} versus D_{min} plot to estimate M_{tc} and N , c) state-dilatancy relationship to estimate χ , and d) G versus p plot to estimate A , and B .

4 TRENDS IN THE MECHANICAL RESPONSE OF MINE TAILINGS

4.1 Critical state line and soil indexes trends

Figure 3 shows the variation of parameters that define the CSLs versus soil index parameters such as fines content (FC), plasticity index (PI), Liquid limit (LL). In these Figures (3a to 3d), we have also added the mine tailings data from Smith et al. (2019). Figure 3a shows the variation λ_e versus FC and Figure 3b shows the variation of the λ_e versus PI . It can be seen that PI is correlated with λ_e ($R^2 = 0.6$ with a better correlation compared to FC), when a material presents a PI . This is expected because both PI and λ_e can be considered as proxies to compressibility. The apparent correlation between PI and λ_e is also consistent with CSSM-based concepts (e.g., see Chapter 6 in Schofield and Wroth, 1968). Hence, this suggests that the common approach of using FC for accounting for compressibility, as it is often done in the cyclic liquefaction assessments for sand materials with fines, may be questionable. PI , on the other hand, is related to the material's mineralogy, which is more fundamentally related to compressibility. This is consistent with the findings from Bray and Sancio (2006), who evaluated the liquefaction triggering of fine-grained soils finding that PI is a better descriptor than FC . Fig. 3c shows the variation of Γ (i.e., the altitude of the CSL at 1kPa for the materials with a linear CSL) versus FC , and Fig. 3d shows the variation of Γ versus $LL \times G_s$.

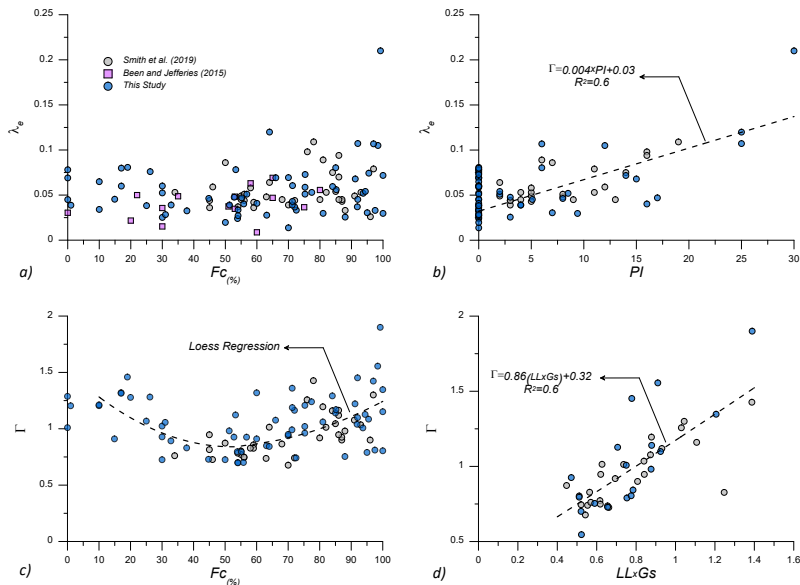


Figure 3. Variation of the CSL slope versus a) FC , and b) PI . Variation of the CSL intercept at 1kPa versus c) FC , and d) $LL \times G_s$.

Figure 3c does not show a strong correlation between Γ and FC , but suggests that Γ tends to decrease with an initial increment of FC , a tendency that is reverted if FC keeps increasing further (note the Loess-based fitting line that illustrates this trend), which is consistent with the findings by previous studies that considered silty sands and sandy silts (e.g., Thevanayagam et al., 2002). Figure 3d evidences a stronger correlation between Γ and $LL \times G_s$. This can be explained as LL

is a measure of the water content of soil at an approximate strength of 2 kPa (Wood, 1991). Considering that shear strength can be normalized, p will be low (for example, if the normalized strength is 0.2, p will be 10 to provide a strength of 2 kPa). The corresponding void ratio can be approximated as the water content (which is represented by LL) times G_s (assuming saturation); hence, by using a semi-logarithmic relationship for the CSL, a linear trend between Γ and LL . G_s is expected (as illustrated in Figure 3d), which is consistent with the findings in Smith et al. (2019). This is also consistent with CSSM concepts, which show a linear correlation between Γ and LL (e.g., see Chapter 6 in Schofield and Wroth, 1968).

4.2 Interpretation of CSL location in terms of particle properties and packing indices

In a broader sense, the altitude and slope of a CSL (i.e., its position) are affected by the overall particle size distribution (e.g., Poulos et al. 1985; Wood and Maeda 2007; Yan and Dong, 2011; Li et al. 2014; Yang and Luo 2017), particle properties (e.g., roundness) as shown by Poulos et al. (1985) and Cho et al. (2006), and mineralogy. To illustrate this, Figure 4a uses the mine tailings data from this study; sands from Cho et al. 2006; and data from Houston sand (HS), glass beads (GB), and DEM simulations from Li et al. 2014. This figure illustrates how the influence of particle properties and grading (using C_u as a proxy) affects the altitude of the CSL. We use Γ_{100} (i.e., the altitude of the CSL at 100 kPa) as it is often better defined than Γ (the altitude at 1 kPa) as discussed in Torres-Cruz and Santamarina (2019). The highlighted data in Fig. 4 are from the Cho et al. (2006) study, where C_u was purposely constrained to a small range to distill the effects of particle shape. Note how Γ_{100} decreases as the roundness increases, and that the Γ_{100} values for particles with lower roundness are within the range observed for mine tailings, which typically have lower roundness due to the processes involved in their generation. Note also how the Γ_{100} from glass beads and DEM simulations (with spherical particles) are consistent with the Γ_{100} for sands with high roundness and lower than Γ_{100} for mine tailings, indicating the role of particle shape. Figure 4b shows the CSL slope (λ_e) variation in terms of C_u considering the mine tailings from this study and the mine tailings from past studies previously described. It is interesting to see how λ_e tends to increase with C_u up to values on the order of 7-8 and then decreases as C_u keeps increasing.

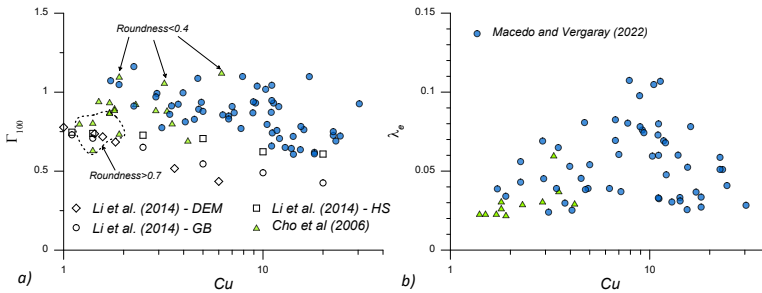


Figure 4. a) Comparison of Γ_{100} vs. C_u and b) λ_e versus C_u for sands (Cho et al. 2006, Li et al. 2014) and mine tailings (see the text for details). HS: Houston Sands, GB: glass beads, DEM: discrete element modeling.

These trends can be interpreted considering the theoretical particle size distributions derived by Lade et al. (1998) that promote enhanced packing (i.e., a low e). Lade et al. (1998) used results from McGery (1961) and found that the e_{min} for binary packing of particles will decrease rapidly as the ratio of coarse and fine particle sizes (D/d) increases up to 7, after which e_{min} keeps decreasing, but at a lower rate; hence, they stated that $D/d = 7$ efficiently creates an enhanced packing. Using this result, Lade et al. (1998) proposed a range for theoretical particle size distribution curves, presented in Figure 5 along with an experimental-based range from McGery (1961). Lade et al. (1998) also defined a “smooth grain size distribution” curve, corresponding to the trend line through the midpoints of the vertical lines (see Fig. 5). Figure 5 also presents the

normalized particle size distributions for the mine tailings in Figure 4. Since the theoretical-based curves from Lade et al. (1998) are dimensionless, the particle sizes were normalized by D_{75} , the size at which 75% of particles are finer, and then scaled for direct comparison. Interestingly, the particle size distributions of the materials with a $C_u > 8$ are generally consistent with the theoretical ranges from Lade et al. (1998), indicating that gradations that result in an enhanced packing may also promote a lower CSL slope as the difference in particle sizes increases (i.e., as C_u increases, using C_u as a proxy for particle sizes). On the other hand, the gradations for materials with $C_u < 8$ are generally not consistent with the theoretical ranges proposed by Lade et al. (1998); hence, they do not favor enhanced packing as the proportion of particle sizes increases (i.e., as C_u increases). Instead, the trend suggests that fine particles may contribute to separating coarser particles, creating looser packing (i.e., a higher CSL slope), which was also suggested by Lade et al. (1998) when the proportion of particle sizes is small (i.e., a low C_u). It is important to emphasize that C_u is used only as a proxy for the proportion of particle sizes, and it is not expected that C_u will capture details of the full particle size distribution or particle-based properties, which is consistent with the significant scatter observed in Fig. 4a and 4b.

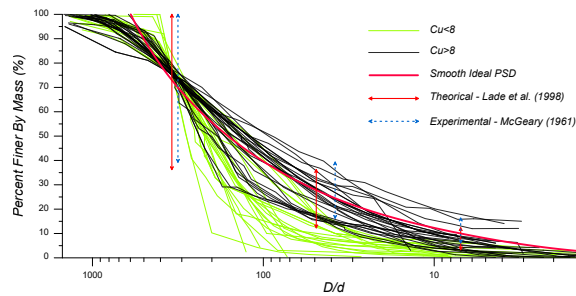


Figure 5. Particle size distributions to produce optimal quaternary packing of spherical particles from Lade et al. (1998) and McGeary (1961) along with the normalized particle size distributions of several tailings (see Section 2 for details).

4.3 Stiffness and Particle size distribution dependence

We explored the stiffness dependence on the particle size distribution of mine tailings using the α and β parameters ($V_s = \alpha (p/1kpa)^\beta$, where V_s is the shear wave velocity from bender tests). Figure 6a and b present the variation of C_u versus α and β , considering the data from this study and the data from Cho et al. (2006) for clean sands (which have a C_u lower than 5).

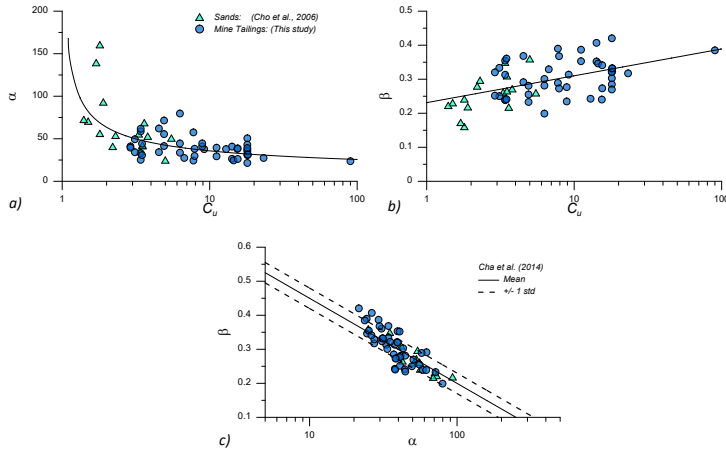


Figure 6. Variation of a) α of b) β and C_u .c) α versus β for mine tailings from this study and sands from Cho et al. (2005)

The trends indicate that as C_u increases α decreases and β increases, this finding is consistent with the observations of Payan et al. (2015) for clean sands and suggest that the overall effect of the irregularities introduced by different particle sizes is to hinder particle mobility and their ability to attain dense packing configurations leading to lower V_s (lower α) that are more susceptible to changes in stresses (higher β). Interestingly, it can also be observed that the trends in mine tailings are consistent with the trends for sands. Figure 6c presents the data of α and β for mine tailings and the trend of Cha et al (2014), who based on a large database of soils (e.g., sands, clays and cemented soils) developed and expression to relate these parameters As shown in Figure 6c the mine tailings values fit very well within the Cha et al (2014) trend, lying in the region between sands and clays and sands. These is expected as mine tailings are silty materials, and the tailings database covers a broad range of FC (0 to 100 %).

4.4 Dilatancy

Figure 7a shows the variation of the maximum dilatancy in triaxial CD tests versus ψ_0 , considering the mine tailings from this study and data available in Jefferies and Been (2016) for sand materials. If we fit the data to the relationship suggested by Been and Jefferies (1985), given by $D_{min} = \chi\psi$ we obtain representative χ values of 3.0 for sands, and 4.0 for tailings. This suggests that mine tailings have an average stronger scaling of dilatancy compared with sands, given a similar state parameter. This can be explained considering that χ can be though as a kinematic parameter related to the potential of particulate materials to re-accommodate particles. Given the higher angularity of mine tailings compared to sands, mine tailings seem to have, on average, a higher potential on re-accommodating particles.

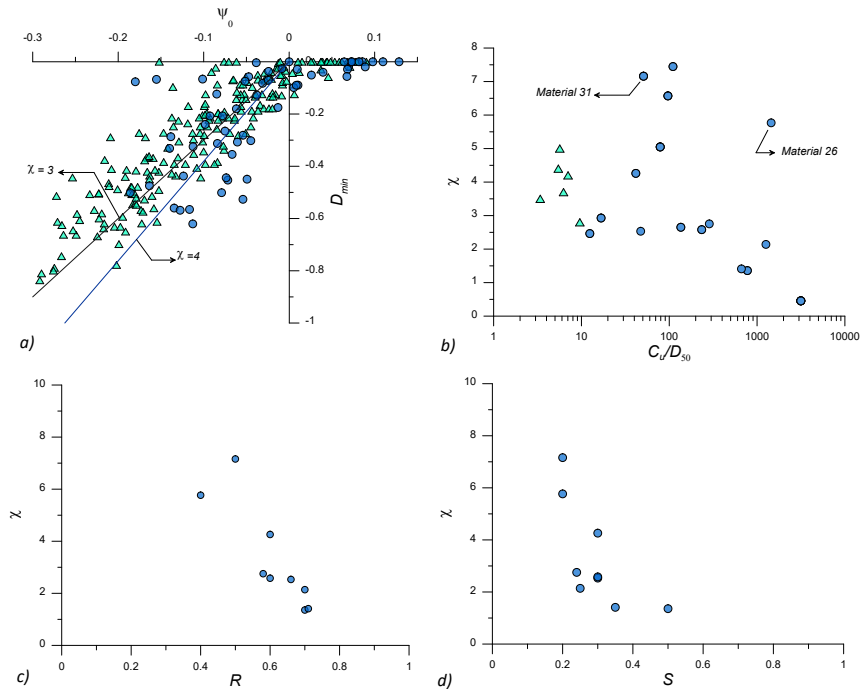


Figure 7. a) Variation of ψ and D_{min} for sands and mine tailings. b) Variation of χ and C_u/D_{50}

Figure 7b shows the variation of χ and C_u/D_{50} for mine tailings and some well-known sand materials (i.e., Erksak, Braster, Changi, Fraser, Nerlek, and Ticino sands). The data for sands was obtained from Jefferies and Been (2016). It can be observed that the χ values in sands vary in a narrow range between 3.5 and 5.0, which correspond to C_u and C_u/D_{50} values that are also in a narrow range (1 to 3, and 3 to 10, respectively). In the case of mine tailings, we observe that χ tends to decrease with the increase of C_u/D_{50} , which is consistent with observations from DEM simulations (Yan and Dong, 2011). We also noticed that the lowest χ values (lower than 1.4) correspond to materials with large FC (larger than 85%) and important clay size fractions. This observation is consistent with the findings from (Cola and Simonini, 2002). The materials 26 and 31 (which correspond to the Cadia and Brumadinho failures previously discussed) showed large χ values (5.8 and 7.2, respectively). These large values may be associated with the large angularity on these materials and bonding effects, although further research is needed to confirm or discard the existence of bonding effects, as suggested by Robertson et al. (2019). Figure 7c and 7d show that χ tends to reduce as roundness (R) and sphericity (S) increase (i.e., angularity decreases), which is consistent with the concept that χ is related the potential of particulate materials to reaccommodate particles.

5 CONCLUSIONS

In this study, we have used critical state soil mechanics (CSSM) concepts to examine salient trends on the mechanical response of mine tailings, highlighting the role of the relative proportions of different particle sizes, and particle properties. Our results suggest that:

- The amount of FC is not a strong proxy to compressibility; hence, its use in liquefaction procedures to bring compressibility effects is questionable. In fine-grained plastic soils, PI seems to be a better proxy since it is related to mineralogy. Bray and Sancio (2006) reached a similar conclusion when evaluating the liquefaction potential in fine-grained soils.
- The theoretical particle size distributions that promote packing proposed by Lade et al. (1998) are useful in understanding general trends for the location of the CSL of mine tailings, highlighting the role of the relative proportions of particle sizes and particle properties.
- The particle gradation influences the small strain shear stiffness and dilatancy, which is consistent with previous observations on sands. An increase in C_u typically reflects on a decrease in α and χ , and an increase in β . The observed trends also suggest that particle shape affects dilatancy, χ tends to decrease as roundness and sphericity increase. The large values χ in mine tailings should be further explored.

6 ACKNOWLEDGEMENTS

This study has been partially funded by the National Science Foundation (NSF) under the CMMI 2013947 project. We also acknowledge the financial support provided by the PRONABEC program of the Peruvian government for the first author.

REFERENCES

- Arroyo, M. and Gens, A. 2021. Computational Analyses of Dam I Failure at the Corrego de Feijao Mine in Brumadinho. Final Report for VALE S.A.
- Been, K. 2016. Characterizing mine tailings for geotechnical design. *Geotechnical and Geophysical Site Characterisation 5*. Australian Geomechanics Society, Sydney, Australia, 41–56.
- Been, K. and Jefferies, M.G. 1985. A state parameter for sands. *Géotechnique*, 35(2):99–112.
- Bray, J.D. and Sancio, R.B. 2006. “Assessment of the liquefaction susceptibility of fine-grained soils.” *Journal of Geotechnical and Geoenvironmental Engineering*, 132(9) 1165–1177.
- Carrera, A., Coop, M., and Lancellotta, R. 2011. Influence of grading on the mechanical behaviour of Stava tailings. *Géotechnique*, 61(11):935–946.
- Cha, M., Santamarina, J. C., Kim, H. S., and Cho, G. C. (2014). Small-strain stiffness, shear-wave velocity, and soil compressibility. *Journal of Geotechnical and Geoenvironmental Engineering*, 140(10), 06014011.
- Cho, G.-C., Dodds, J., Santamarina, J.C. (2006). “Particle Shape Effects on Packing Density, Stiffness, and Strength: Natural and Crushed Sands.” *Journal of Geotechnical and Geoenvironmental Engineering*, 132(5):591–602. Available at: [http://dx.doi.org/10.1061/\(asce\)1090-0241\(2006\)132:5\(591\)](http://dx.doi.org/10.1061/(asce)1090-0241(2006)132:5(591)).
- Cola, S., and Simonini, P. 2002. Mechanical behavior of silty soils of the Venice lagoon as a function of their grading characteristics. *Canadian Geotechnical Journal*, 39(4):879–893.
- Fotovat, A., Sadrekarimi, A., and Etehad, M. 2022. Instability of Gold Mine Tailings subjected to Undrained and Drained Unloading Stress Paths. *Géotechnique*. 1-51. 10.1680/jgeot.21.00293.
- Fourie, A.B. and Tshabalala, L. 2005. Initiation of static liquefaction and the role of K0 consolidation. *Canadian Geotechnical Journal*, 42(3):892–906.
- Hardin, B.O., and Richart, F.E. 1963. Elastic wave velocities in granular soils. *Journal of the Soil Mechanics and Foundations Division, ASCE*, 89(SM1):33-65.
- Jefferies, M.G., 1993. Nor-Sand: a simple critical state model for sand. *Géotechnique*, 43(1):91–103.
- Jefferies, M. G. and Been, K. 2016. Soil liquefaction: a critical state approach, 2nd edn. Boca Raton, FL, USA: *CRC Press*.
- Jefferies, M. (2022). “Improving governance will not be sufficient to avoid dam failures.” Proceedings of the Institution of Civil Engineers – Geotechnical Engineering, 1–15. Doi:10.1680/jgeen.21.00105
- Kossoff, D., Dubbin, W.E., Alfredsson, M., Edwards, S.J., Macklin, M.G., Hudson-Edwards, K.A. (2014). “Mine tailings dams: Characteristics, failure, environmental impacts, and remediation.” *Applied Geochemistry*, 51, 229–245. Doi:10.1016/j.apgeochem.2014.09.010
- Lade, P., Liggio, C., Yamamoto, J. (1998). “Effects of non-plastic fines on minimum and maximum void ratios of sand.” *Geotechnical Testing Journal*, 21(4), 336. Doi:10.1520/gtj11373j
- Li, G., Liu, Y.-J., Dano, C., Hicher, P.-Y. (2014). “Grading-Dependent Behavior of Granular Materials: From Discrete to Continuous Modeling.” *Journal of Engineering Mechanics*, 141(6), 04014172. Doi:10.1061/(asce)em.1943-7889.0000866
- Macedo, J., Bray, J., Olson, S., Bareither, C., and Arnold, C. (2020). TAILENG mine tailings database. Tailings and mine waste 2020 conference, Keystone, Colorado.
- Macedo, J., Vergaray, L. (2021). “Properties of Mine Tailings for Static Liquefaction Assessment.” *Canadian Geotechnical Journal*. Doi:10.1139/cgj-2020-0600
- McGeary, R. K. (1961). “Mechanical Packing of Spherical Particles.” *Journal of the American Ceramic Society*, 44(10), 513–522. Doi:10.1111/j.1151-2916.1961.tb13716.x
- Morgenstern, N.R. (2018). “Geotechnical Risk, Regulation, and Public Policy – The Sixth Victor de Mello Lecture.” *Soils and Rocks*, 41(2):107-129.
- Morgenstern, N. R., Jefferies, M., Zyl, D., and Wates, J. 2019. Independent Technical Review Board. Report on NTSF Embankment Failure. Ashurst Australia.
- Morgenstern, N. R., Vick, S. G., Viotti, C. B., and Watts, B. D. 2016. Fundao tailings dam review panel. Report in the immediate causes of the failure of the Fundao Dam. New York: Cleary Gottlieb Steen and Hamilton LLP. Available at: <http://fundaoinvestigation.com/the-panel-report/>.
- Pestana, J.M. and Whittle, A.J. 1995. Compression model for cohesionless soils. *Géotechnique*, 45(4):611–631.
- Poulos, S.J., Castro, G., France, J.W. (1985). “Liquefaction Evaluation Procedure.” *Journal of Geotechnical Engineering*, 111(6), 772–792. Doi:10.1061/(asce)0733-9410(1985)111:6(772)
- Rabbi, A.T.M.Z., Rahman, M.M., and Cameron, D.A. 2019. The relation between the state indices and the characteristic features of undrained behaviour of silty sand. *Soils and Foundations*, 59(4):801–813.
- Robertson, P.K., De Melo, L., Williams, D.J., and Wilson, G.W. 2019. Report of the Expert Panel on the Technical Causes of the Failure of Feijão Dam I.
- Sadrekarimi, A. 2014. Effect of the mode of shear on static liquefaction analysis. *Journal of Geotechnical and Geoenvironmental Engineering*, 140(12):04014069.

- Santamarina, J.C., Torres-Cruz, L.A., Bachus, R.C. (2019). "Why coal ash and tailings dam disasters occur." *Science*, 364(6440), 526–528. Doi:10.1126/science.aax1927
- Schofield, A. and Wroth, C.P. 1968. "Critical State Soil Mechanics." McGraw-Hill, ISBN: 978-0641940484.
- Shuttle, D. and Jefferies, M. 2016. Determining silt state from CPTu. *Geotechnical Research*, 3(3):90–118.
- Smith, K., Fanni, R., Capman, P., Reid, D. 2019. Critical State Testing of Tailings: Comparison between Various Tailings and Implications for Design. *Proceedings of Tailings and Mine Waste*. Vancouver.
- Thevanayagam, S., Shenthan, T., Mohan, S., and Liang, J. 2002. "Undrained Fragility of Clean Sands, Silty Sands, and Sandy Silts." *Journal of Geotechnical and Geoenvironmental Engineering*, 128(10):849–859.
- Torres-Cruz, L.A. and Santamarina, J.C. (2019). "The critical state line of non-plastic tailings." *Canadian Geotechnical Journal*, pp.1–10. Available at: <http://dx.doi.org/10.1139/cgj-2019-0019>.
- Wood, D.M. 1991. "Soil behaviour and critical state soil mechanics." Cambridge University Press.
- Wood, M.D., Maeda, K. (2007). "Changing grading of soil: effect on critical states." *Acta Geotechnica*, 3(1), 3–14. Doi:10.1007/s11440-007-0041-0
- Yan, W. M., and Dong, J. 2011. Effect of Particle Grading on the Response of an Idealized Granular Assemblage. *International Journal of Geomechanics*, 11(4):276–285.
- Yang, J., and Luo, X. D. (2017). "The critical state friction angle of granular materials: does it depend on grading." *Acta Geotechnica*, 13(3), 535–547. Doi:10.1007/s11440-017-0581-x